Salinomycin inhibits breast cancer progression via targeting HIF-1α/VEGF mediated tumor angiogenesis *in vitro* and *in vivo*

Jayant Dewangan[a], Sonal Srivastava[a], Sakshi Mishra[a], Aman Divakar[a], Sadan Kumar[b], Srikanta Kumar Rath[a,*]

[a] Genotoxicity Lab, Division of Toxicology and Experimental Medicine, CSIR-Central Drug Research Institute, Lucknow 226031, Uttar Pradesh, India
[b] Immunotoxicity Lab, Division of Toxicology and Experimental Medicine, CSIR-Central Drug Research Institute, Lucknow 226031, Uttar Pradesh, India

ARTICLE INFO

ABSTRACT

Cancer is a complex disease wherein cells begin to divide abnormally and spread into surrounding tissues. Angiogenesis plays a crucial role in tumor progression as it is required for sustained growth and metastasis, therefore targeting angiogenesis is a promising therapeutic approach for breast cancer management. Salinomycin (SAL) has been reported to exhibit anticancer response on various types of cancer. In the present study, we explored the antiangiogenic and anticancer efficacy of the polyether ionophore SAL in the breast cancer model. It effectively inhibited cell proliferation, invasion, and migration. It also inhibited the expression of pro-angiogenic cell surface marker CD31 in HUVEC, thereby interrupting the endothelial tubulogenesis. It decreased the HIF-1α transcription factor DNA binding activity to HRE sequence in HUVEC and human breast cancer cells. Further, corresponding to our *in vitro* findings, SAL suppressed neovascularization in the chick chorioallantoic membrane and the Matrigel plug implanted mice model. Bioluminescence and immuno-fluorescence imaging revealed that SAL treatment in mice inhibits breast cancer growth and tumor angiogenesis. SAL also suppressed the serum VEGFA level in tumor-bearing mice and induced caspase-dependent apoptosis in breast cancer cells. Taken together our findings suggested that SAL inhibits VEGF induced angiogenesis and breast cancer growth via interrupting HIF-1α/VEGF signalling and could be used as a promising antiangiogenic agent for breast cancer treatment.

1. Introduction

Cancer is the potent cause of mortality in men and women worldwide. According to GLOBOCAN report, 18.1 million cancer incidence and 9.6 million deaths were estimated due to cancer in 2018. Among female, breast cancer accounts for 24% of all cancer cases and 15% of all cancer-associated deaths that reached to 626,679 mortality in women in the year 2018 [1,2]. Therapies available for the management of breast cancer are surgery, radiotherapy, chemotherapy, immunotherapy, targeted therapy, hormonal therapy, and stem cell transplantation. Despite the remarkable enhancement in the understanding and management of breast cancer in the past few years, it remains a major health risk and poses significant challenges [3].

Angiogenesis, the formation of new blood vessels from already existing vessels, plays an intricate role in tumor growth, progression and metastasis [4]. Antiangiogenic therapies not only potentiate tumor regression and metastasis but also have several advantages over conventional chemotherapy. Few antiangiogenic drugs have been

approved by the FDA and are currently being used for the treatment of breast cancer; nonetheless, some adverse effects have been associated with their long-term use [5]. Therefore, a search for a safe and novel antiangiogenic agent is extremely warranted.

Salinomycin (SAL) is a monocarboxylic polyether ionophore, obtained from *Streptomyces albus*, and is known to possess antibacterial, antifungal, antiparasitic, antiviral, anti-inflammatory and anticancer activities [6]. Studies have revealed that SAL has the efficacy to selectively target breast cancer stem cells and to sensitize drug-resistant cells to chemotherapeutic drugs [7]. It is very effective either alone or in combination therapy with natural compounds and exhibits its antiproliferative effect by various mechanisms in different cancers [8]. SAL has been shown to exhibit its effect via modulating Stat3, autophagy, NF-kB, P-glycoprotein, EMT, Wnt signalling, ER stress oxidative stress, disrupting membrane potential and inducing caspase-mediated apoptosis [9,10].

In the present study, Human Umbilical Vein Endothelial Cells (HUVECs) and Human Breast Cancer Cells (HBCCs) MCF-7 and MDA-

---

MB-231 have been used to explore the effect of SAL on angiogenesis and cancer. Endothelial cell (EC) proliferation, migration, and differentiation were studied on an *in vitro* model system, whereas, *in vivo* validation was carried out in chick Chorioallantoic Membrane (CAM) and Matrigel plug implanted mice model. Our results also demonstrated that SAL inhibited angiogenesis and breast cancer progression by inhibiting HIF-1α/VEGF/VEGFR2 signalling axis and inducing caspase-dependent apoptosis pathways.

2. Materials and methods

2.1. Materials

Salinomycin, Sulforhodamine B (SRB), cholera endotoxin and hydrocortisone were purchased from Sigma Aldrich Co. (Sigma, St. Louis, MO, USA). Recombinant human VEGF, EGF, DMEM/F12, RPMI-1640, penicillin-streptomycin solution, horse serum, fetal bovine serum (FBS), NE-PER™ nuclear and cytoplasmic extraction kit, VEGF mouse ELISA kit, and Cell Event™ caspase-3/7 green detection kit, were procured from Thermo Fisher Scientific (Grand Island, NY, USA). Cytochrome *C* release apoptosis assay kit was acquired from BioVision Incorporated (Milpitas, USA). Annexin V-FITC apoptosis kit and Matrigel were purchased from BD Biosciences (San Jose, CA, USA). HIF-1α Transcription Factor Assay Kit was obtained from Cayman Chemicals (Ann Arbor, USA). Antibodies were procured against CD31 (MA5-16337) from Thermo Fisher Scientific; Cyclin D1 (C7464) from Sigma-Aldrich; active caspase-3 (3015-100), Bcl-2 (3033-100) from BioVision; actin (sc-1616) from Santa Cruz (Texas, USA); VEGFA (NB100-664) from Novus Biologicals (Littleton, USA); HIF-1α (3716S), VEGF Receptor 2 (2472S), cleaved caspase-7 (9491T), Bax (5023T), HSP60 (12165T) from Cell Signaling Technologies (Beverly, MA, USA).

2.2. Cell culture and treatments

HUVEC was purchased from HiMedia Laboratories and cultured in endothelial cell expansion medium for not more than ten passages. MCF-7, MDA-MB-231, and MCF-10A cells were procured from the American Type Culture Collection, USA and were used below twenty passage. T-47D, MDA-MB-468, and HEK-293 cells were obtained from National Centre for Cell Sciences, Pune, India. Luciferase and GFP reporter tagged 4T1 cells was procured from Perkin Elmer. MCF-7, MDA-MB-231, MDA-MB-468, and HEK-293 were maintained in DMEM/F12 whereas, T-47D and 4T1 were propagated in RPMI 1640. MCF-10A cells was cultured as described earlier [11]. All the cells were grown in the presence of gentamicin (50 μg/ml), penicillin (100 U/ml), streptomycin (100 μg/ml) and 10% FBS, and maintained in a humidified CO_2 incubator at 37 °C. For experiments, HBCCs were treated in complete medium for 24 h. However, to study the VEGF induced angiogenesis, HUVEC were starved for 8 h followed by drug treatment in medium containing 10 ng/ml VEGF. Hypoxia was induced by treating the cells with 150 μM $CoCl_2$ for 5 h which stabilizes the HIF-1α and serves as hypoxia-mimicking agent [11].

2.3. Cytotoxicity studies

Approximately 7×10^3 cells were plated in 96 well plates and incubated at 37 °C. The cells were exposed to different concentrations of SAL for 24 h. Cells were fixed with trichloroacetic acid followed by staining with Sulforhodamine B (SRB). Cell-bound SRB was dissolved in Tris base, and absorbance was recorded at 510 nm using SpectraMaxM2^{e}Elisa Microplate Reader (Molecular Devices Inc.).

2.4. Wound healing assay

Wound healing was studied to assess the effect of SAL on cell migration. 0.2×10^6 MCF-7, MDA-MB-231, and HUVEC were plated in 6 well plates. About 90% confluence, cells were serum starved for 8 h followed by which a wound was created by scratching the cells using 10 μl tip. Cells were treated with indicated concentrations of SAL in the complete growth medium. In the case of HUVEC, treatment was given in medium containing 10 ng/ml VEGF. The image was captured at 0 and 12 h using Nikon's Eclipse TS100 microscope (Japan) and wound closure were measured using Nikon Documentation Imaging Software.

2.5. Boyden chamber cell invasion assay

The cellular invasion was monitored with the help of a Boyden chamber cell culture insert. In the study, pre-starved cells were seeded in serum-free medium on Matrigel-coated transwell having a pore size of 8 μm (Corning, NY, USA). The lower chamber contains a chemoattractant (10% serum for breast cancer cells and VEGF for HUVEC). Transwell was washed with PBS and incubated in cell dissociation buffer (Gibco, Thermo Fisher Scientific) containing Calcein AM. Fluorescence of invaded cells was recorded at 495 nm excitation/ 515 nm emission using fluorimeter.

2.6. Endothelial cell proliferation assay

HUVEC was cultured in 96 well black plates with a clear bottom and incubated at 37 °C. Next day cells were nutrient starved for 8 h. Cells were then treated with SAL in medium supplemented with 10 ng/ml VEGF for 24 h. Cells were washed with 1x PBS after treatment period then incubated with Calcein AM for 30 min in the dark. Fluorescence was recorded at 495 nm excitation/515 nm emission.

2.7. Tube formation assay

SAL mediated anti-angiogenic response *in vitro* was evaluated by assessing the interruption of HUVECs to form a tube-like structure in the presence of SAL. On Matrigel-coated 24 well plate, 4×10^4 pre-starved HUVECs were seeded and incubated at 37 °C until tube-like structures were formed (about 16 h). Cells were stained with Calcein AM dye and photographed under a fluorescence microscope (Nikon, Japan).

2.8. Immunocytochemistry of CD31

HUVECs were grown on a coverslip and treated with SAL for 24 h. Cells were fixed with 3.7% paraformaldehyde and permeabilized with 0.2% Triton X-100. For immunostaining, cells were blocked with 2% BSA followed by overnight incubation with CD31 primary antibody at 4 °C. After washing, it was incubated with Alexa Fluor 488 conjugated secondary antibody. For microscopic examination images were acquired with a fluorescence microscope (Carl Zeiss). A flow cytometric analysis further validated data in different sets of experiments.

2.9. Chorioallantoic membrane assay

Chick CAM angiogenesis assay was performed as described previously [11]. Fertilized chicken eggs were collected and incubated at 37 °C under constant humidity. On the 7th day, one small hole was created on the blunt end of eggs where the air sac is present. Using suction method, the air was sucked out from air sac to evade attachment of the embryo to the upper cortex. Subsequently, a $2 \times 1\, cm^2$ window was created on eggshell to expose CAM. SAL along with VEGF was absorbed on gelatin sponge and placed over CAM. Windows were sealed and incubated for four more days. After the incubation period, the eggshell was opened to monitor sprouting and blood vessel density. Images were acquired by Nikon stereo zoom microscope.

2.10. Matrigel plug assay

Matrigel plug assay was performed to study angiogenesis *in vivo*. About 400 µl Matrigel was mixed with 100 ng VEGF and SAL, and injected subcutaneously in Balb/c mice. Two weeks after the injection, mice were sacrificed, and Matrigel plug was excised out. Matrigel plug was photographed and processed for histological analysis. Angiogenesis was monitored by hematoxylin-eosin staining and immunohistochemistry of CD31.

2.11. HIF-1α transcription factor activity

HIF-1α transcription factor activity assay was performed according to the manufacturer's protocol (Cayman Chemicals, Michigan, USA). Briefly, the cytosolic/nuclear protein was isolated from 2.5 and 5 µM SAL treated cells using the NE-PER™ Nuclear and Cytoplasmic Extraction Kit. Nuclear extract was mixed with complete transcription factor binding assay buffer and added to HIF-1α dsDNA sequence coated 96 well plates for overnight binding. After washing, HIF-1α primary antibody was added followed by incubation with HRP conjugated secondary antibody. Finally, the developer solution added, and absorbance was recorded at 450 nm.

2.12. Estimation of mouse VEGF level by ELISA

VEGF-A level was measured in the serum sample of 4T1 tumor-bearing mice (n = 4). Blood samples were collected from SAL -treated mice after 21 days of treatment. Serum was isolated and stored at −80 °C until further use. The experiment was performed as directed by the manufacturer's protocol (Thermo Fisher Scientific). Briefly, 100 µl of diluted serum sample was incubated in antibody-coated wells for 2.5 h and washed for four times to remove unbound VEGF. Next, 100 µl of biotinylated antibody was poured followed by incubation with the streptavidin-HRP reagent. After 45 min, the TMB substrate was added to each well and absorbance was recorded at 450 nm.

2.13. Annexin V/PI binding assay

Cells were plated in 6 well plates at a density of 0.2×10^6 cells per well. Cells were treated with 2.5–10 µM of SAL for further 24 h. Cells were trypsinized and labelled with Annexin V FITC and PI (Becton Dickinson, USA) and incubated for 15 min at room temperature. Labelled cells were acquired in a flow cytometer (BD FACS Calibur).

2.14. Alteration in mitochondrial membrane potential (MMP)

Mitochondrial damage upon treatment with SAL was analyzed by flow cytometer using a cell-permeable dye, JC-1. Briefly, cells were trypsinized and plated in 6 well plates at a density of 0.2×10^6 cells per well. Next day, cells were treated with assigned doses of SAL for 24 h. Cells were harvested and incubated with 2.5 µg/ml JC-1 fluorescent dye for 15 min at 37 °C in the dark before the acquisition. Change in MMP was analyzed using flow cytometer and represented as a ratio of red: green fluorescence.

2.15. Cytochrome c release assay

Cytochrome *c* (Cyt c) release assay was performed according to the manufacturer's protocol (BioVision, USA). Briefly, control and SAL-treated cells were suspended in 200 µl Cytosolic Extraction Buffer containing DTT and protease inhibitor. The cells were incubated on ice for 10 min, sonicated and centrifuged at $10,000 \times g$ for 30 min at 4 °C. The supernatant was labeled as the Cytosolic Fraction. The pellet was re-suspended in 100 µl of Mitochondrial Extraction Buffer. The sample was vortexed, and the tubes were labeled as Mitochondrial Fraction. 10 µg of protein proceeded with the standard protocol of western blot

using anti-Cytochrome-c antibody.

2.16. Caspase 3/7 activity

Activation of caspase 3/7 was analyzed using CellEvent™ Caspase-3/7 Green Detection Reagent by flow cytometer. Briefly, 0.2×10^6 cells were plated in 6 well culture plate, and the next day treated with 2.5, 5 and 10 µM of SAL for 24 h. After the treatment period, cells were incubated with caspase 3/7 antibody using the CellEvent™ Caspase-3/7 green detection reagent (C10427, Thermo Fisher Scientific) for 30 min at 37 °C in the dark. Caspase activity was measured by flow cytometer.

2.17. In vivo tumor regression

The animal study was conducted according to the guidelines as well as the protocols approved by the Institutional Animal Ethics Committee (IAEC; approval no: IAEC/2016/3) CSIR–CDRI, Lucknow, India. Briefly, 4T1 (5×10^6) cells were inoculated subcutaneously beneath the mammary pad of female Balb/c mice (weight 20 ± 2 g). When tumor size was considerable, the mice were randomly divided into 3 groups (n = 6). Mice were treated with vehicle or SAL (5 mg/kg and 10 mg/kg body weight) intraperitoneally, three days in a week for a total three weeks. Tumor volume was measured by vernier caliper using formula Tumor volume V $(mm^3) = \pi/6$ (Length) $\times$ (Width)^2. For *in vivo* imaging of tumor, XenoLight RediJect D-Luciferin was injected in mice then anesthetized isoflurane inhalation and imaged with In Vivo Imaging System (IVIS Spectrum, Caliper Life Sciences). Mice were sacrificed by CO_2 inhalation, and tumors were excised and photographed. Tumor samples were fixed in formalin and processed for histological analysis.

2.18. Western blotting

Western blotting was performed as described previously [12]. SAL treated cells were lysed using cell lysis buffer (Cell Signalling Technologies) and quantified by Bradford reagent at 595 nm absorbance. Equal protein was loaded on SDS PAGE and subsequently transferred onto PVDF membrane. Blocking was performed by incubating membrane in 5% BSA for 1 h at room temperature. The membrane was washed with PBST (PBS + 0.1% Tween 20) followed by primary and HRP conjugated secondary antibody incubation. Finally, the blot was developed in a chemidoc system using enhanced chemiluminescence detection reagent.

2.19. Statistical analysis

The results were expressed as Mean ± SD performed in triplicate. One way Analysis of Variance (ANOVA) was used to analyze the significance of data by applying Bonferroni's Multiple Comparison Test. Statistically significant difference was defined as P < 0.05.

3. Results

3.1. SAL induced cytotoxic response in HBCCs

SAL induced cytotoxic response was studied by SRB assay after 24 h of treatment. SAL reduced the cellular viability of HBCCs (MCF-7, MDA-MB-234, T-47D, and MDA-MB-468) and mouse breast adenocarcinoma 4T1 cells. However, non-tumorigenic human breast epithelial cells MCF-10A and human embryonic kidney cells HEK-293 were comparatively least affected at the lower doses. This study supports the selective cytotoxic response of SAL towards breast cancer cells (Fig. 1).

3.2. SAL inhibited migration and invasion of EC and HBCCs

These assays were performed to assess the effect of unidirectional
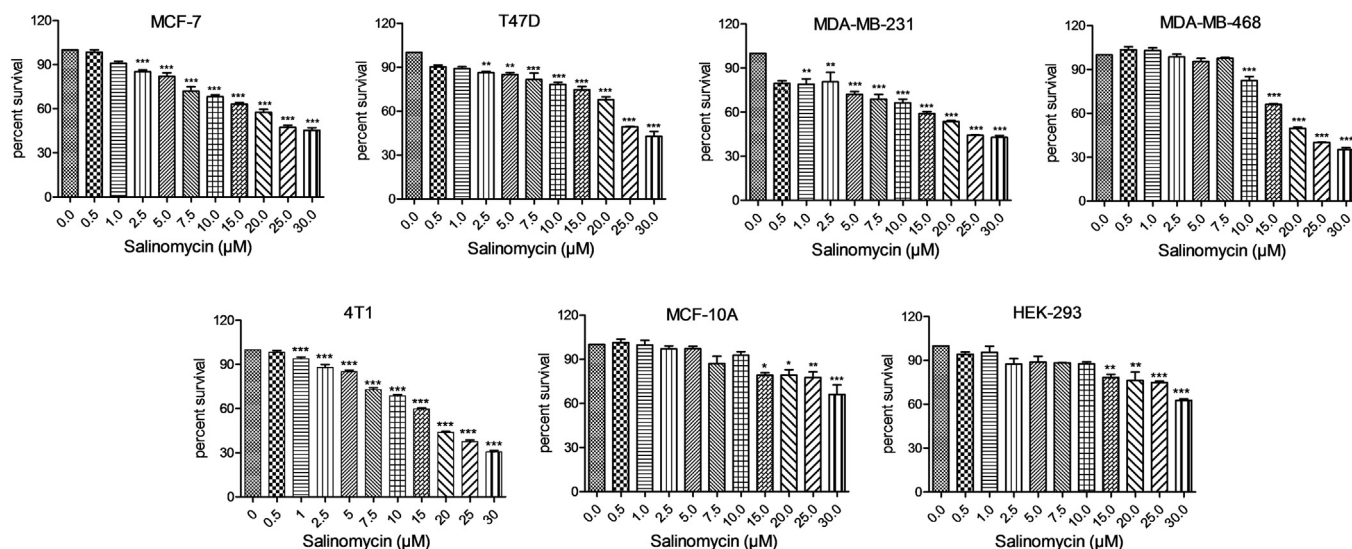
Fig. 1. SAL inhibits proliferation of HBCCs. Cells were treated with SAL for 24 h, and cell viability was measured on MCF-7, T47D, MDA-MB-231, MDA-MB-468, 4T1, MCF-10A and HEK-293 by SRB assay. Experiments were carried out in three independent repeats and results were expressed as % of control, mean ± SD. Significance was represented as * $P < 0.05$; ** $P < 0.01$; *** $P < 0.001$ compared to control.
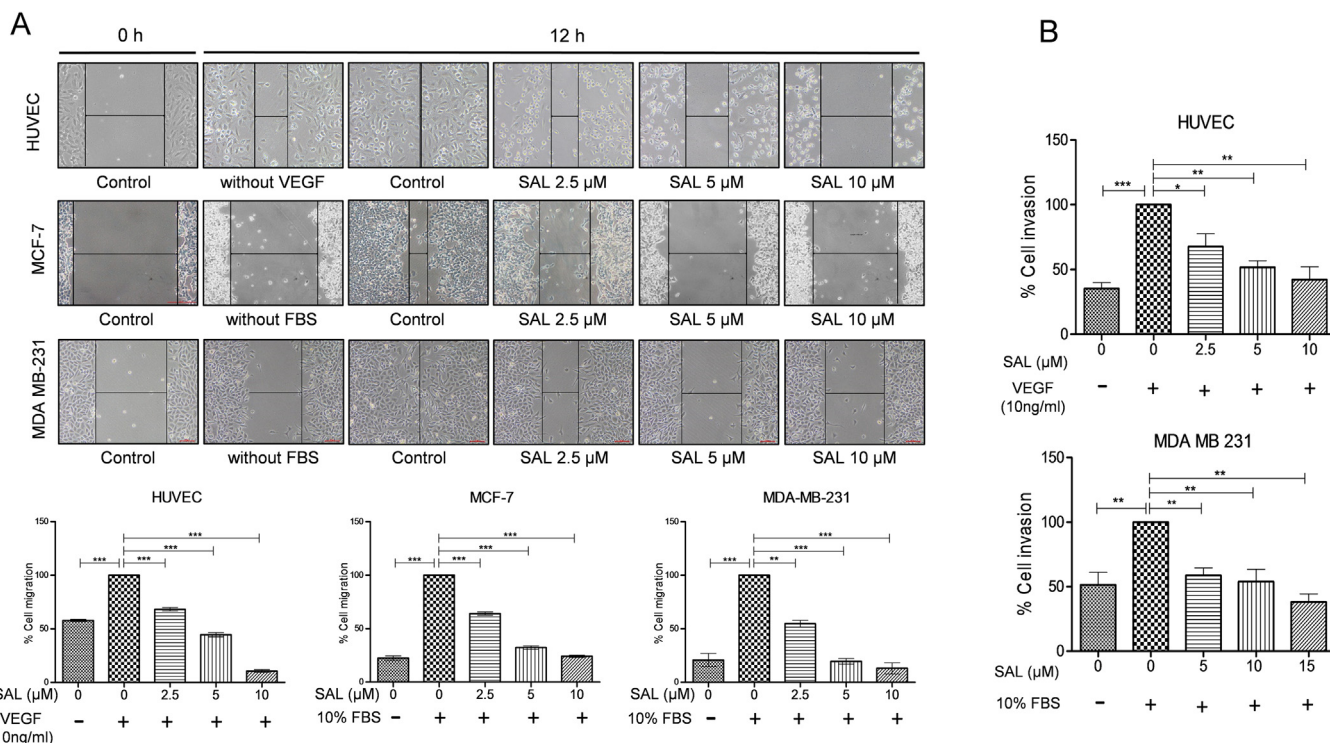
Fig. 2. SAL reduces cell migration and invasion. A. Wound healing assay was executed to check the migration of HUVEC, MCF-7, and MDA-MB-231 cells after SAL treatment. A wound has been created on confluent cells and images were acquired at zero hour and twelve-hour time point. B. Cell invasion assay was performed on Matrigel-coated cell culture insert. Invaded cells were incubated in cell dissociation buffer containing Calcein AM followed by fluorescence was recorded. Cell migration and invasion were measured and presented as a percent to control with FBS/VEGF. Significance was represented as mean ± SD (n = 3), * $P < 0.05$; ** $P < 0.01$; *** $P < 0.001$.

migration of cells either in the presence of a growth factor or test compound. One wound was created on confluent cells, and cells were allowed to migrate for 12 h. SAL treatment significantly reduced the migration ability of HUVEC, MCF-7 and MDA-MB-231 cells. Similarly, SAL reduced the invasiveness of HUVEC and MDA-MB-231 cells. The assay was not performed in MCF-7, as it has a poor invasive phenotype. SAL also prevented VEGF-induced migration and invasion of EC which suggests that SAL has anti-migratory and anti-invasive potential (Fig. 2A, B).

3.3. SAL inhibited EC proliferation and tubulogenesis

Calcein AM is the non-fluorescent dye which permeates live pro-liferating cells and gets hydrolysed by esterases to form fluorescent Calcein. SAL significantly inhibited HUVEC proliferation, as lower Calcein-AM fluorescence intensity was recorded in SAL treated group (Fig. 3A). In order to evaluate whether the proliferation inhibition was due to apoptosis Annexin V/PI staining in the HUVEC was performed. Fig. 3D depicts that no significant apoptosis induction was observed in
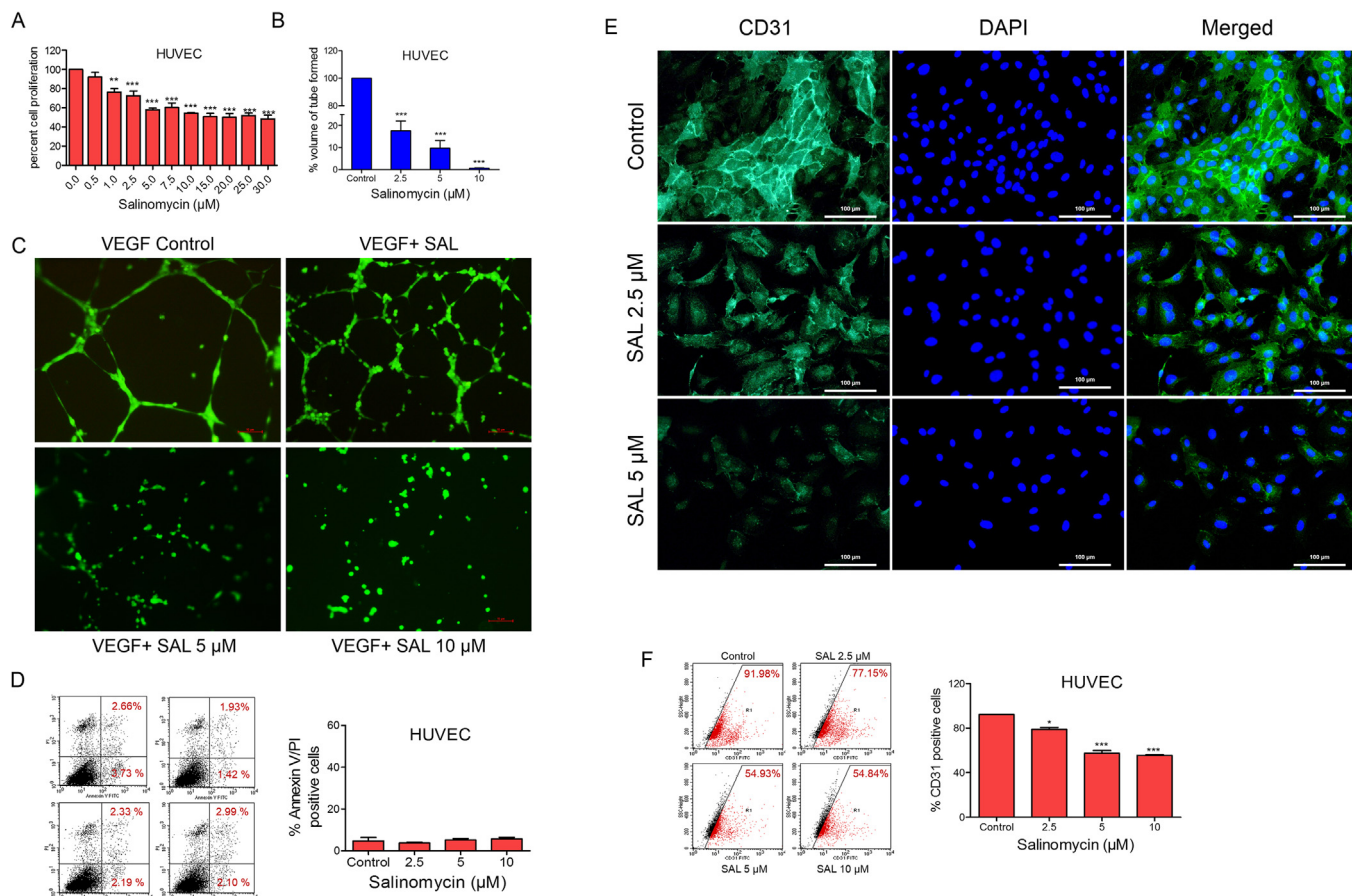
Fig. 3. SAL inhibits EC proliferation and differentiation. A. Endothelial cell proliferation was monitored by Calcein AM fluorescent dye. SAL dose-dependently inhibited HUVEC proliferation. B & C. SAL inhibited HUVEC tube formation. HUVEC was differentiated on extracellular matrix and formed tube-like structure which was stained with Calcein AM and photographed with a fluorescence microscope. D. SAL mediated apoptosis on HUVEC was monitored by Annexin V FITC and propidium iodide staining. E & F. SAL treatment inhibited the Platelet endothelial cell adhesion molecule or CD31 required for tube formation. Immunofluorescence of CD31 was monitored by fluorescence microscope and flow cytometer. All the bar graph represents results as respect to control, mean ± SD. Significance was represented as * $P < 0.05$; ** $P < 0.01$; *** $P < 0.001$ compared to control.

the endothelial cells due to SAL treatment. When HUVEC was cultured on Matrigel, under a nutrient-starved condition *in vitro,* it differentiated and formed tubular structures. VEGF induced large size tube formation in HUVEC and served as a positive control. SAL significantly reduced the tubular area and number of tubes formed in HUVEC thereby inhibiting tube forming potential (Fig. 3B, C).

3.4. SAL reduced CD31 expression in HUVEC

CD31 or Platelet endothelial cell adhesion molecule (PECAM) is a well-known pro-angiogenic marker. This surface marker expression was evaluated by microscopic examination and flow cytometry. Immunostaining images exhibited less fluorescence intensity in SAL treated HUVEC compared to VEGF-induced control cells. Similar results were obtained in flow cytometric analysis where maximum CD31 positive population was observed in control cells (about 91%). However, SAL treatment significantly reduced this population to 54%. The results confirmed that SAL has the ability to remarkably repress the expression of CD31 on HUVECs surface (Fig. 3E, F).

3.5. SAL inhibited angiogenesis in ovo and in vivo

The anti-angiogenic potential of SAL was evaluated *in ovo* on the chorioallantoic membrane of fertilized chick eggs. SAL was placed over CAM, and it was observed that SAL significantly reduced vessel sprouting. However, more vessel branching was visualized in the VEGF

treated group (Fig. 4A). Similarly, the antiangiogenic response was evaluated *in vivo* on Balb/c mice by subcutaneously injecting Matrigel. VEGF treated plug was observed with more blood vessels and appeared more reddish because of higher vessel sprouting. Whereas, VEGF + SAL treated plug had fewer blood vessels and appeared less reddish as compared to VEGF control. Angiogenesis was monitored by immunohistochemistry using endothelial marker CD31 (Fig. 4B).

3.6. SAL inhibited HIF-1α transcription factor activity

HIF-1α transcription factor activity was studied by measuring this transcription factor binding potential to a specific double-stranded DNA sequence containing the HIF-1α response element (5′-ACGTG-3′). Nuclear extract of SAL treated HUVEC, MCF-7 and MDA-MB-231 were incubated in the HIF-1α ds DNA coated plate. SAL significantly reduced HIF-1α activity in all of these cells under both hypoxic and normoxic conditions. However, its activity was found to be more pronounced under hypoxia as compared to normoxia (Fig. 5A).

3.7. SAL inhibited hypoxia-induced HIF-1α/VEGF signaling axis

HIF-1α protein is oxygen sensitive and gets degraded under normoxic condition. Hypoxia stabilizes HIF levels; however, SAL inhibited hypoxia-induced HIF-1α expression in EC and HBCCs. It also suppressed the VEGFA level in HBCCs and its receptor VEGFR2 expression present on the surface of HUVEC (Fig. 5B). VEGFA level was also

A   Chick Chorioallantoic assay model
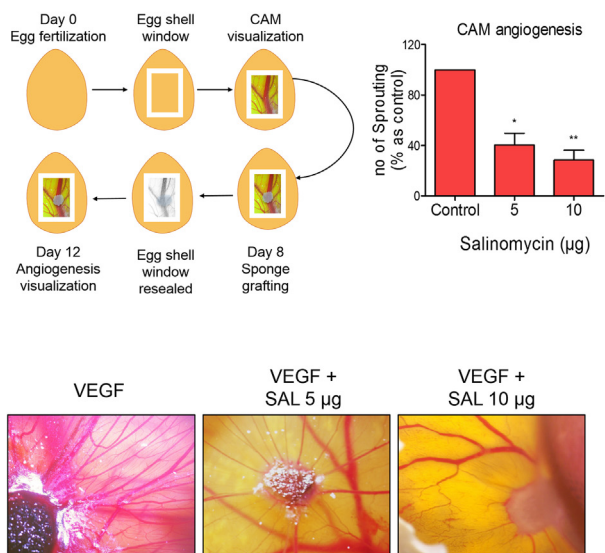
B   Mice Matrigel plug assay
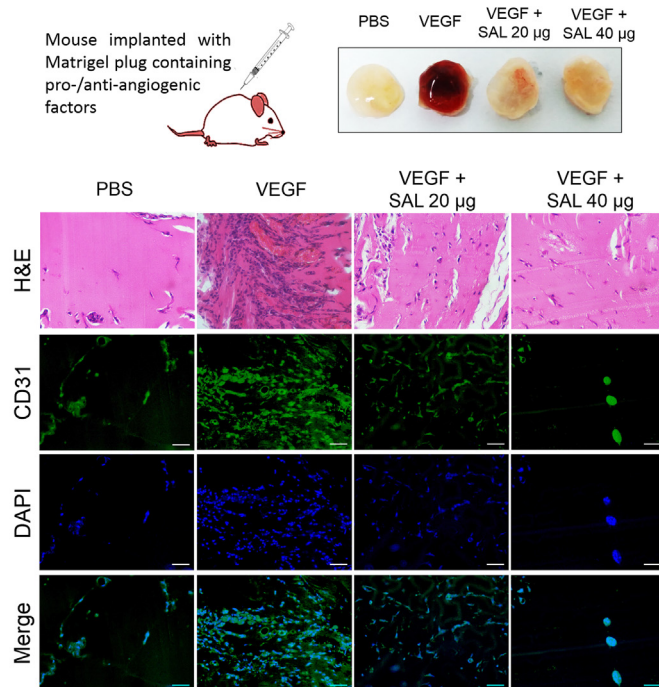
Fig. 4. SAL suppresses angiogenesis *in ovo* and *in vivo*. A. SAL inhibits VEGF induced vessel sprouting in chick CAM *in ovo*. The image was photographed by a stereo zoom microscope, and vessel sprouting was counted. The experiment was performed in three repeats. Significance was measured as mean ± SD, * P < 0.05; ** P < 0.01; *** P < 0.001 in comparison to control. B. Effect of SAL on neovascularization was studied *in vivo* in Balb/c mice (n = 3). Extracellular matrix was implanted subcutaneously in mice for two weeks. End of the study, mice were sacrificed, and plugs were photographed. Matrigel plug was processed for H&E and immunofluorescence staining for CD31 to study the angiogenesis.
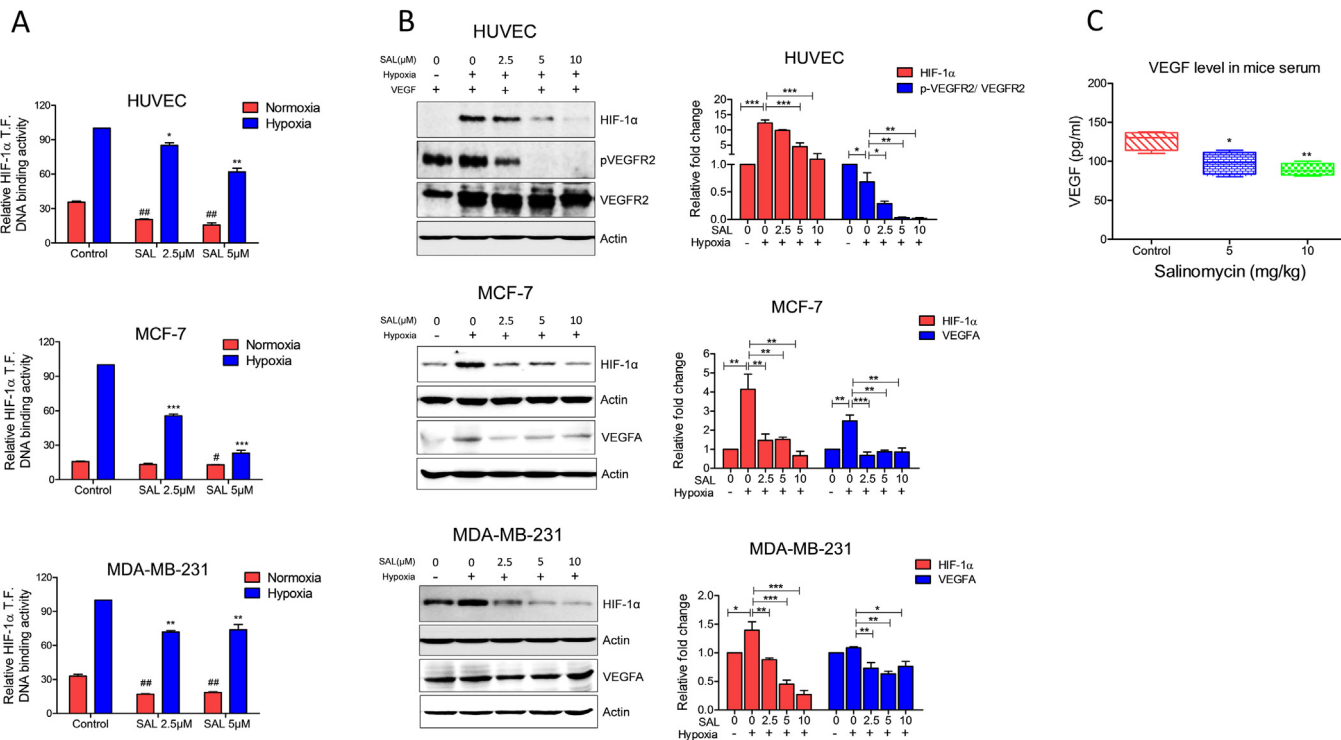
Fig. 5. SAL inhibits HIF-1α/VEGF/VEGFR2 signalling axis in EC and HBCCs. A. SAL inhibited DNA binding activity of HIF-1α transcription factor to hypoxia response elements of HUVEC, MCF-7 and MDA-MB-231 cells under hypoxic and normoxic conditions. Experiment was performed in triplicates and significance was measured as mean ± SD, # P < 0.05; ## P < 0.01; ### P < 0.001 comparison to control in normoxia; * P < 0.05; ** P < 0.01; *** P < 0.001 comparison to control in hypoxia. B. SAL inhibits HIF-1α and VEGF in HBCCs, and their receptor expression in EC. Experiments were carried out in triplicates and data presented are mean ± SD, * P < 0.05; ** P < 0.01; *** P < 0.001. C. Mouse VEGF ELISA was performed to monitored serum VEGFA level in SAL treated mice (n = 4).
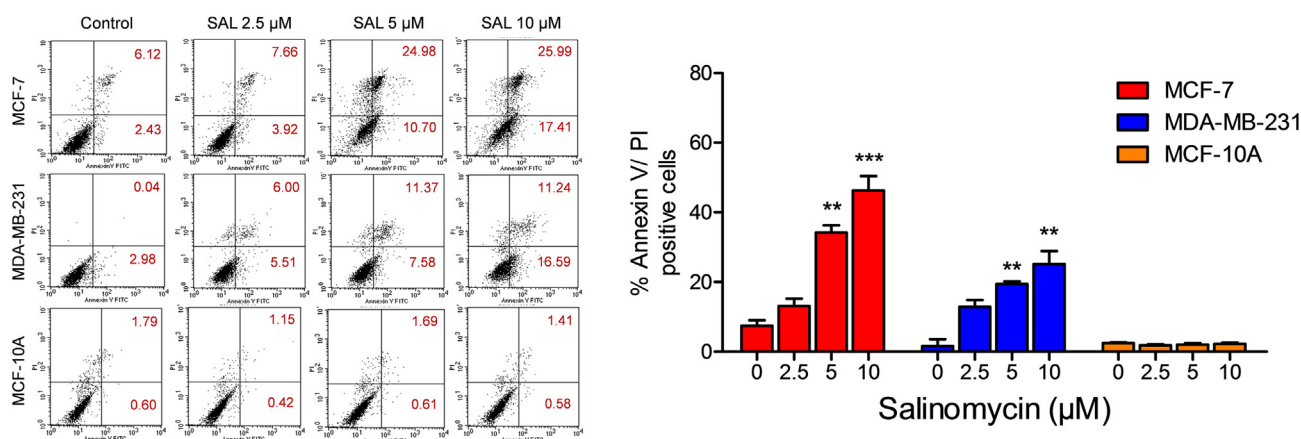
Fig. 6. SAL selectively induces apoptosis in HBCCs. Cells were treated with SAL for 24 h followed by labelled with Annexin V FITC/propidium iodide and acquired in a flow cytometer. SAL induced apoptosis in MCF-7 and MDA-MB-231 breast cancer cells; however, human mammary epithelial cells MCF-10A was remained unaffected at selected dose. experiments were performed in three independent repeats and significance was measured as mean ± SD, * $P < 0.05$; ** $P < 0.01$; *** $P < 0.001$ compared to control.

monitored in ELISA in the serum of tumor-bearing Balb/c mice. Mice receiving 5 mg/kg and 10 mg/kg of SAL exhibited a significant reduction in serum VEGF level as compared to the vehicle-treated group (Fig. 5C).

3.8. SAL selectively induced apoptosis in HBCCs

SAL mediated apoptotic response was studied by Annexin V/PI staining using flow cytometer. SAL dose-dependently induced apoptosis in both the HBCCs after 24 h of treatment. MCF-7 is more sensitized to SAL compared to MDA-MB-231 as the percentage of Annexin V/PI positive cells was more in MCF-7 cells. However, non-tumorigenic breast epithelial cell MCF-10A remained unaffected by the SAL treatment, indicated their safety towards normal cells (Fig. 6).

3.9. SAL disrupts MMP and induces Cyt c release from mitochondria

Mitochondrial membrane potential in MCF-7, MDA-MB-231 and MCF-10A was examined using JC-1 fluorescent dye. In HBCCs, untreated cells were found with higher JC-1 aggregates, which produce red fluorescence. However, SAL treated cells had a significant increase in JC-1 monomeric form, which emits green fluorescence. MCF-10A cells were least affected by SAL treatment. Alteration in membrane potential was represented as a ratio of JC-1 red: green fluorescence (Fig. 7A). Change in MMP leads to Cyt c release from the inner mitochondrial membrane during the early stages of apoptosis. SAL treatment decreased mitochondrial Cyt c in HBCCs and elevated its cytosolic levels. The results suggest that SAL induced a mitochondrial-dependent cell death pathway (Fig. 7B).

3.10. SAL triggers caspase 3/7 activation in HBCCs

Caspases are a family of endoproteases which play a pivotal role in apoptosis and cell death regulation. Caspase assay was performed to explore the apoptotic pathway. Flow cytometer detected active form of caspases inside the cells. The result demonstrated that SAL induced caspase activation dose-dependently in both the HBCCs. 10 μM of SAL treatment activated 70% and 56% caspase 3/7 in MCF-7 and MDA-MB-231 cells respectively. However, SAL could not significantly induce active-caspase level in MCF-10A cells. Western blot expression analysis also supported caspase activation in HBCCs, since MCF-7 is deficient in caspase-3, so caspase-7 is the effector caspase in it. Further, treatment increased expression of pro-apoptotic protein Bax and decreased the anti-apoptotic factor Bcl2 and cyclin D1 in both the HBCCs (Fig. 7C, D).

3.11. SAL suppressed tumor growth in the 4T1 mouse model

In vivo tumor regression was monitored in 4T1 breast cancer cells induced tumor model. The tumor growth was significantly reduced in animals treated with SAL (5 mg/kg & 10 mg/kg) as compared to the vehicle-treated group. Tumor volume was measured with the help of Vernier Calipers and recorded twice a week. Tumor size was also monitored by bioluminescence imaging via *in vivo* imaging system (IVIS Spectrum, Caliper Life Sciences). Fig. 8A–C illustrated the significant reduction of tumor growth in SAL-treated groups. Tumors sections were labelled with endothelial specific marker CD31 which indicated the extent of angiogenesis is reduced with SAL treatment (Fig. 8D).

4. Discussion

The cells in tumor divide continuously; therefore, they require a continuous blood supply to proliferate. Inhibiting neo-vasculature formation from existing vessels cuts the supply of nutrients and other essentials required by the tumor thereby limiting tumor growth thus, making it a primary target for the anti-angiogenic agent [13]. Anti-angiogenic therapy should be explored in the treatment of breast cancer as it offers a novel approach to target breast cancer.

SAL, a polyether ionophore antibiotic is a known anti-neoplastic agent and has been demonstrated to effectively and selectively eliminate cancer stem cells [7]. It is an emerging anticancer molecule and useful in the treatment of various cancers by acting different mechanisms. It promotes differentiation and apoptosis in acute promyelocytic leukemia cells [14]. SAL is a very good modulator of autophagic flux in cancer cells provoking cell death [15]. A recent report showed that SAL inhibits gastric cancer growth by reversal of multidrug resistance via targeting epithelial-mesenchymal transition associated long noncoding RNA [16]. A previous study suggested that SAL inhibits VEGFR2 mediated angiogenesis in a gastric cancer xenograft mouse model by hampering tyrosine kinase activity of the VEGF receptor and STAT3 signalling pathway in endothelial cells [17]. However, its anti-angiogenic potential has not yet been fully explored. Herein, we have studied different molecular aspects of its anticancer potential as well as its employment as an antiangiogenic agent to target breast cancer cells.

The present study comprised the screening of SAL over different types of cells. MCF-7, T-47D are ER-positive; MDA-MB-231 and MDA-MB-468 are human triple negative; 4T1 is the mouse triple-negative breast cancer cells. However, human mammary epithelial cells MCF-10A and human embryonic kidney HEK-293 cells were used as non-tumorigenic epithelial cells (Fig. 1). Cell proliferation and migration have a great impact on angiogenesis process making these suitable
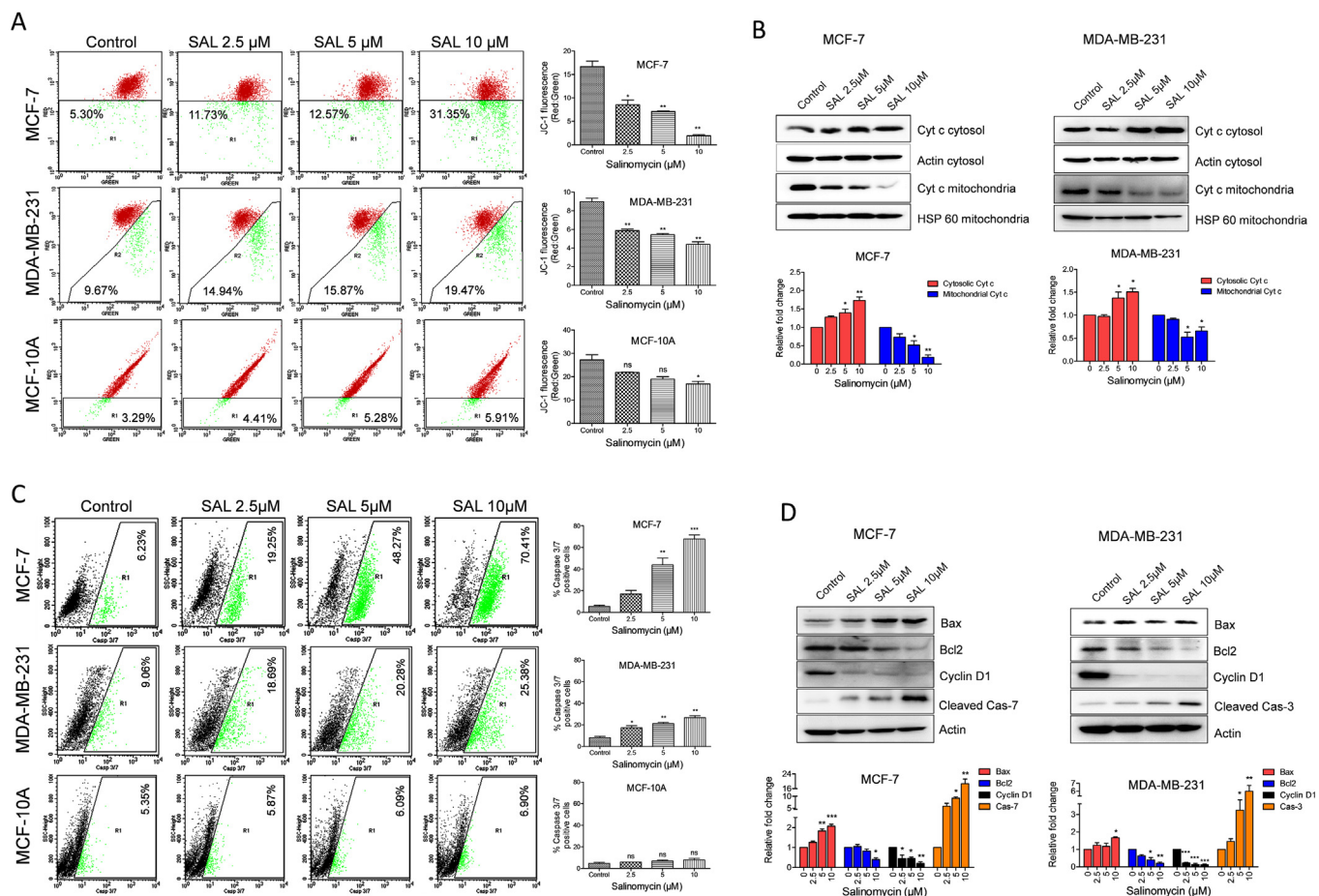
Fig. 7. SAL alters MMP and mitochondrial-dependent caspase activation. A. Effect of SAL on mitochondrial membrane depolarization was measured on a flow cytometer using JC1 dye. B. Cyt. c release assay was performed on a mitochondrial and cytosolic fraction of SAL treated HBCCs. Actin and HSP 60 was used as a loading control for cytosolic and mitochondrial protein respectively. C. SAL treatment enhanced caspase 3/7 activity in MCF-7 and MDA-MB-231 cells, not in MCF-10A. D. Western blots of anti and pro-apoptotic factors involved in SAL mediated HBCCs death. All the experiments were performed in three independent repeats and significance was measured as mean ± SD, * $P < 0.05$; ** $P < 0.01$; *** $P < 0.001$ compared to control.
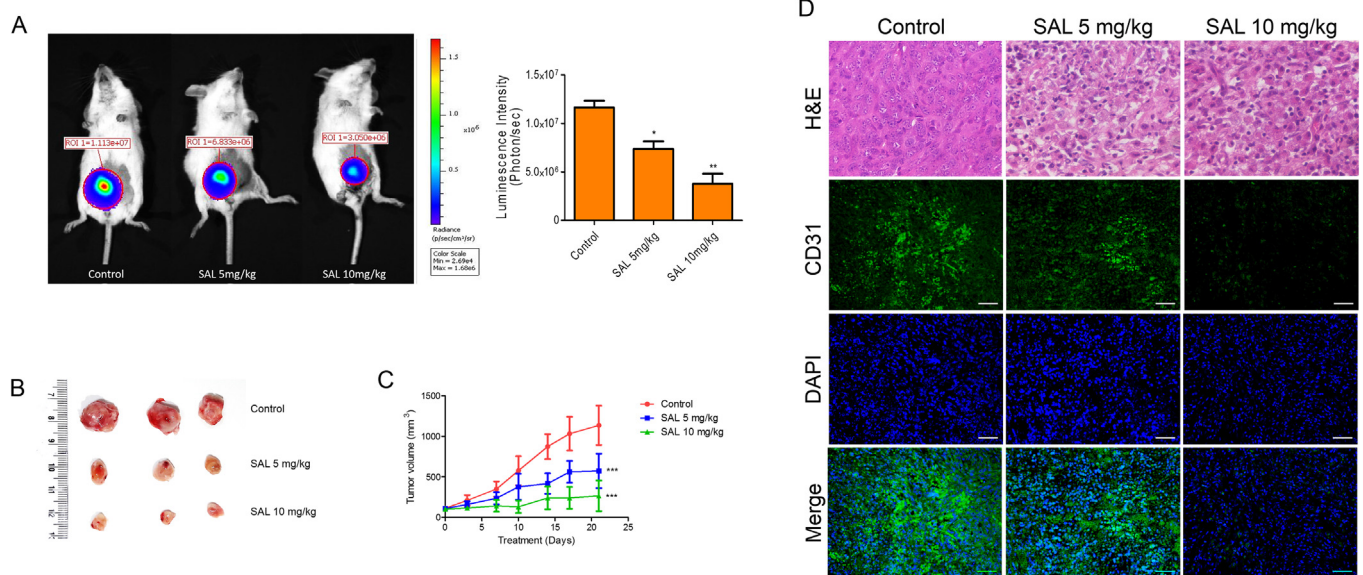
Fig. 8. SAL inhibits breast cancer progression in 4T1 mice model. A. Tumor-bearing mice were treated with 5 mg/kg and 10 mg/kg SAL for 21 days, and tumor regression was monitored with luminescence imaging using live animal imaging system. Luminescence intensity was plotted in the graph. B–D. The tumor was excised photographed and processed for histological examinations. IHC of CD31 performed on breast tumor section to study the angiogenesis *in vivo*. SAL treatment inhibits breast tumor angiogenesis. Data presented are mean ± SD, * $P < 0.05$; ** $P < 0.01$; *** $P < 0.001$ in comparison to control group.

targets in the anti-angiogenic regime [18]. SAL inhibited cell migration and invasion in many cancers like prostate cancer [19], lung cancer [20], endometrial cancer [21] and destabilized matrix metalloproteinases [22]. HUVEC under nutrient-deprived conditions morphologically differentiates and forms capillary-like structure. When it is cultured over basement membrane extract in growth factor reduced medium, HUVEC starts aggregating to create tubule, which mimics *in vivo* like capillary formation process [23]. Platelet endothelial cell adhesion molecule or CD31 is an essential marker of angiogenesis which localizes into intercellular junctions of endothelial cells. Inhibition of CD31 results in retardation of tube formation and neovascularization by inhibiting the interaction between endothelial cells [24]. Our study explored that SAL inhibited proliferation, migration, and invasion of breast cancer and EC. It also prevented VEGF-induced tube formation in HUVECs by decreasing CD31 expression (Figs. 2 and 3).

CAM assay has been extensively used to study angiogenesis, and also offers an attractive alternative to mice model for the assessment of new anti-angiogenic agents [25]. Similarly, Matrigel plug assay is an *in vivo* approach to assess angiogenesis in mice model. Matrigel is the extracellular matrix obtained from Englebreth-Holm-Swarm sarcoma which resembles the environment found in human tissues. The extent of angiogenesis was monitored by embedding and sectioning the plugs in paraffin followed by Hematoxylin & Eosin staining [26]. In our study, SAL inhibited the neovascularization *in ovo* and *in vivo* (Fig. 4).

Studies have shown that HIF-1α is the master regulator of angiogenesis signalling pathways. This transcription factor (TF) is a member of the basic helix-loop-helix family of TFs and plays an eminent role in maintaining cellular oxygen homeostasis [27,28]. HIF-1α has emerged as an important TF in breast cancer biology and is expressed in the early stages of mammary carcinogenesis. Under hypoxic conditions, HIF-1α forms a heterodimer with HIF-1β and gets translocated into the nucleus, where it binds to the promoter of hypoxia-responsive genes. Hypoxia stabilizes HIF-1α expression, whereas, in normoxia, it degrades via ubiquitination process [29]. The present study revealed that SAL rendered HIF-1α TF activity by inhibiting their binding to dsDNA of HIF-1α response element. The activity is suppressed in the nuclear extract of HUVEC, MCF-7 and MDA-MB-231 cells under both normoxic and hypoxic conditions (Fig. 5A, B).

VEGF is one of the essential growth factors which promotes microvessel density and breast cancer angiogenesis. It is also a highly specific mitogen for endothelial cells. VEGF binding to their receptor activates signal transduction resulting in endothelial proliferation, migration, and neovascularization. Solid tumors secrete VEGF to promote angiogenesis and their growth. Circulating VEGF level is the prognostic marker for the increased tumor growth and metastatic spread. Increased serum VEGF in cancer patients is usually associated with unresponsive chemotherapy, disease progression and poor survival [30–32]. SAL also reduced the serum VEGFA level in tumor-bearing mice (Fig. 5C).

Evasion of apoptosis is one of the major hallmarks of cancer due to which tumor cell population expands in number [33]. SAL induces cell death in various types of cancer viz. breast, hepatic, lung, prostate, leukemia, and ovarian cancer by triggering apoptotic cascade [9]. It induced apoptosis in MCF-7 and MDA-MB-231 breast cancer cells not in non-tumorigenic mammary epithelial cells MCF-10A (Fig. 6). Some other safety studies also supported the use of SAL in cancer treatment. Scherzad et al. performed genotoxicity studies of SAL on lymphocytes and nasal mucosa cells, and found to be safe [34]. SAL does not alter the immunophenotyping and differentiation ability of human bone marrow mesenchymal stem cells. It shows little cytotoxic response above the 30 μM doses [35]. Mitochondrial dysfunction and loss of membrane potential play a central role in the apoptosis pathway, resulting in the release of certain mitochondrial apoptogenic factors such as cytochrome *c* during apoptosis [36]. SAL disrupted Δψ$_m$ in both the HBCCs and potentiated the release of cytochrome *c* from the mitochondrial membrane to the cytosol (Fig. 7A, B). Proteins of the Bcl2 family

actively participate in mitochondrial death signaling through cytochrome *c* release. The release of cytochrome *c* activated the caspase cascade to act via a proteolytic cleavage that brings multiple cellular changes leading to apoptosis [37]. Further, SAL treatment increased Bax: Bcl2 ratio in HBCCs (Fig. 7C, D). At lower doses, SAL significantly does not change MMP in non-tumorigenic MCF-10A cells while 10 μM of SAL decreased the JC-1 ratio (p < 0.05). However, this change was not enough to trigger caspase activation and thereby apoptosis.

The results obtained from *in vitro* studies were further validated *in vivo* using 4T1- syngeneic mouse model. The results of the present study confirmed that SAL at an intraperitoneal dose of 5 mg/kg and 10 mg/kg significantly reduced tumor volume. The tumor growth was also measured using Luc-tagged 4T1 bioluminescence imaging system where the treatment significantly reduced photon counts indicating a reduced tumor size (Fig. 8). Together, these studies suggest that SAL inhibited breast cancer progression and exhibited a robust anti-angiogenic response which may be associated with inhibition of HIF-1α/VEGF signalling. This study delivers influential substantiation for the clinical development of SAL as an antiangiogenic agent for the treatment of breast cancer and other solid tumors.

Conflict of interests

The authors declare that there are no conflicts of interest.

References

[1] World Health Organization, 2018. http://www.who.int/cancer/prevention/diagnosis-screening/breast-cancer/en/.
[2] F. Bray, J. Ferlay, I. Soerjomataram, R.L. Siegel, L.A. Torre, A. Jemal, Global cancer statistics 2018: GLOBOCAN estimates of incidence and mortality worldwide for 36 cancers in 185 countries, CA Cancer J. Clin. 68 (6) (2018) 394–424.
[3] K.E. Lukong, Understanding breast cancer – the long and winding road, BBA Clin. 7 (2017) 64–77.
[4] M.C. Chen, C.F. Lee, W.H. Huang, T.C. Chou, Magnolol suppresses hypoxia-induced angiogenesis via inhibition of HIF-1alpha/VEGF signaling pathway in human bladder cancer cells, Biochem. Pharmacol. 85 (9) (2013) 1278–1287.
[5] F. Elice, F. Rodeghiero, Side effects of anti-angiogenic drugs, Thromb. Res. 129 (Suppl 1) (2012) S50–S53.
[6] A. Huczynski, J. Janczak, M. Antoszczak, J. Wietrzyk, E. Maj, B. Brzezinski, Antiproliferative activity of salinomycin and its derivatives, Bioorg. Med. Chem. Lett. 22 (23) (2012) 7146–7150.
[7] P.B. Gupta, T.T. Onder, G. Jiang, K. Tao, C. Kuperwasser, R.A. Weinberg, E.S. Lander, Identification of selective inhibitors of cancer stem cells by high-throughput screening, Cell 138 (4) (2009) 645–659.
[8] J. Dewangan, D. Tandon, S. Srivastava, A.K. Verma, A. Yapuri, S.K. Rath, Novel combination of salinomycin and resveratrol synergistically enhances the anti-proliferative and pro-apoptotic effects on human breast cancer cells, Apoptosis Int. J. Programmed Cell Death 22 (10) (2017) 1246–1259.
[9] J. Dewangan, S. Srivastava, S.K. Rath, Salinomycin: a new paradigm in cancer therapy, Tumour Biol. J. Int. Soc. Oncodev. Biol. Med. 39 (3) (2017) 1010428317695035.
[10] C. Naujokat, R. Steinhart, Salinomycin as a drug for targeting human cancer stem cells, J. Biomed. Biotechnol. 2012 (2012) 950658.
[11] J. Dewangan, S. Kaushik, S.K. Rath, A.K. Balapure, Centchroman regulates breast cancer angiogenesis via inhibition of HIF-1alpha/VEGFR2 signalling axis, Life Sci. 193 (2018) 9–19.
[12] J. Dewangan, S. Srivastava, S. Mishra, P.K. Pandey, A. Divakar, S.K. Rath, Chetomin induces apoptosis in human triple-negative breast cancer cells by promoting calcium overload and mitochondrial dysfunction, Biochem. Biophys. Res. Commun.

495 (2) (2018) 1915–1921.

[13] N. Nishida, H. Yano, T. Nishida, T. Kamura, M. Kojiro, Angiogenesis in Cancer, Vascular Health Risk Manage. 2 (3) (2006) 213–219.

[14] Y. Zhao, L. Zhong, L. Liu, S.F. Yao, M. Chen, L.W. Li, Z.L. Shan, C.L. Xiao, L.G. Gan, T. Xu, B.Z. Liu, Salinomycin induces apoptosis and differentiation in human acute promyelocytic leukemia cells, Oncol. Rep. 40 (2) (2018) 877–886.

[15] J. Jiang, H. Li, E. Qaed, J. Zhang, Y. Song, R. Wu, X. Bu, Q. Wang, Z. Tang, Salinomycin, as an autophagy modulator– a new avenue to anticancer: a review, J. Exp. Clin. Cancer Res. CR 37 (1) (2018) 26.

[16] Z. Mao, Y. Wu, J. Zhou, C. Xing, Salinomycin reduces epithelial-mesenchymal transition-mediated multidrug resistance by modifying long noncoding RNA HOTTIP expression in gastric cancer cells, Anticancer Drugs (2019).

[17] T. Li, X. Liu, Q. Shen, W. Yang, Z. Huo, Q. Liu, H. Jiao, J. Chen, Salinomycin exerts anti-angiogenic and anti-tumorigenic activities by inhibiting vascular endothelial growth factor receptor 2-mediated angiogenesis, Oncotarget (2016).

[18] K.A. Norton, A.S. Popel, Effects of endothelial cell proliferation and migration rates in a computational model of sprouting angiogenesis, Sci. Rep. 6 (2016).

[19] K. Ketola, M. Hilvo, T. Hyotylainen, A. Vuoristo, A.L. Ruskeepaa, M. Oresic, O. Kallioniemi, K. Iljin, Salinomycin inhibits prostate cancer growth and migration via induction of oxidative stress, Br. J. Cancer 106 (1) (2012) 99–106.

[20] K. Arafat, R. Iratni, T. Takahashi, K. Parekh, Y. Al Dhaheri, T.E. Adrian, S. Attoub, Inhibitory Effects of Salinomycin on Cell Survival, Colony Growth, Migration, and Invasion of Human Non-Small Cell Lung Cancer A549 and LNM35: Involvement of NAG-1, PloS one 8(6) (2013) e66931.

[21] S. Kusunoki, K. Kato, K. Tabu, T. Inagaki, H. Okabe, H. Kaneda, S. Suga, Y. Terao, T. Taga, S. Takeda, The inhibitory effect of salinomycin on the proliferation, migration and invasion of human endometrial cancer stem-like cells, Gynecol. Oncol. 129 (3) (2013) 598–605.

[22] D. Wu, Y. Zhang, J. Huang, Z. Fan, F. Shi, S. Wang, Salinomycin inhibits proliferation and induces apoptosis of human nasopharyngeal carcinoma cell in vitro and suppresses tumor growth in vivo, Biochem. Biophys. Res. Commun. 443 (2) (2014) 712–717.

[23] Y. Kubota, H.K. Kleinman, G.R. Martin, T.J. Lawley, Role of laminin and basement membrane in the morphological differentiation of human endothelial cells into capillary-like structures, J. Cell Biol. 107 (4) (1988) 1589–1598.

[24] H.M. DeLisser, M. Christofidou-Solomidou, R.M. Strieter, M.D. Burdick, C.S. Robinson, R.S. Wexler, J.S. Kerr, C. Garlanda, J.R. Merwin, J.A. Madri,

S.M. Albelda, Involvement of endothelial PECAM-1/CD31 in angiogenesis, Am. J. Pathol. 151 (3) (1997) 671–677.

[25] D. Ribatti, Chicken chorioallantoic membrane angiogenesis model, Methods Mol. Biol. 843 (2012) 47–57.

[26] K.M. Malinda, In vivo matrigel migration and angiogenesis assay, Methods Mol. Biol. 467 (2009) 287–294.

[27] G.L. Wang, B.H. Jiang, E.A. Rue, G.L. Semenza, Hypoxia-inducible factor 1,, is a basic-helix-loop-helix-PAS heterodimer regulated by cellular O2 tension, PNAS 92 (12) (1995) 5510–5514.

[28] M. Safran, W.G. Kaelin, HIF hydroxylation and the mammalian oxygen-sensing pathway, J. Clin. Investig. 111 (6) (2003) 779–783.

[29] K.S. Kimbro, J.W. Simons, Hypoxia-inducible factor-1 in human breast and prostate cancer, Endocr. Relat. Cancer 13 (3) (2006) 739–749.

[30] A. Hoeben, B. Landuyt, M.S. Highley, H. Wildiers, A.T. Van Oosterom, E.A. De Bruijn, Vascular endothelial growth factor and angiogenesis, Pharmacol. Rev. 56 (4) (2004) 549–580.

[31] M. Toi, K. Inada, H. Suzuki, T. Tominaga, Tumor angiogenesis in breast cancer: its importance as a prognostic indicator and the association with vascular endothelial growth factor expression, Breast Cancer Res. Treat. 36 (2) (1995) 193–204.

[32] R.T. Poon, S.T. Fan, J. Wong, Clinical implications of circulating angiogenic factors in cancer patients, J. Clin. Oncol. Official J. Am. Soc. Clin. Oncol. 19 (4) (2001) 1207–1225.

[33] D. Hanahan, R.A. Weinberg, The hallmarks of cancer, Cell 100 (1) (2000) 57–70.

[34] A. Scherzad, S. Hackenberg, C. Schramm, K. Froelich, C. Ginzkey, R. Hagen, N. Kleinsasser, Geno- and cytotoxicity of salinomycin in human nasal mucosa and peripheral blood lymphocytes, Toxicol. in vitro Int. J. Published Assoc. BIBRA 29 (4) (2015) 813–818.

[35] A. Scherzed, S. Hackenberg, K. Froelich, K. Rak, A. Technau, A. Radeloff, U. Noth, C. Koehler, R. Hagen, N. Kleinsasser, Effects of salinomycin on human bone marrow-derived mesenchymal stem cells in vitro, Toxicol. Lett. 218 (3) (2013) 207–214.

[36] X. Liu, C.N. Kim, J. Yang, R. Jemmerson, X. Wang, Induction of apoptotic program in cell-free extracts: requirement for dATP and cytochrome c, Cell 86 (1) (1996) 147–157.

[37] D. Hanahan, R.A. Weinberg, Hallmarks of cancer: the next generation, Cell 144 (5) (2011) 646–674.